INTERNATIONAL JOURNAL OF
COASTAL & OFFSHORE ENGINEERING
IJCOE Vol.4/No. 2/Summer 2019 (11-29)

Available online at: http://ijcoe.org/browse.php?a_code=A-10-72-2&sid=1&slc_lang=en

A Probability Distribution Model for the Degree of Bending In Tubular KT-Joints of Offshore Jacket-Type Platforms Subjected To IPB Moment Loadings

Hamid Ahmadi[1*], Vahid Mayeli[2], Esmaeil Zavvar[3]

[1] *Faculty of Civil Engineering, University of Tabriz; h-ahmadi@tabrizu.ac.ir*
[2] *Faculty of Civil Engineering, University of Tabriz; mayeli.vahid@gmail.com*
[3] *Faculty of Civil Engineering, University of Tabriz; esmaeilzavvar@gmail.com*

ARTICLE INFO

Article History:
Received: 5 Mar. 2019
Accepted: 1 Sep. 2019

Keywords:
Tubular KT-joint
Fatigue
Degree of bending (DoB),
Probability density function (PDF)
Kolmogorov-Smirnov test

ABSTRACT

The objective of present research was the derivation of probability density functions (PDFs) for the degree of bending (DoB) in tubular KT-joints commonly found in jacket-type platforms. A total of 243 finite element (FE) analyses were carried out on 81 FE models of KT-joints subjected to three types of in-plane bending (IPB) moment loading. Generated FE models were validated using experimental data, previous FE results, and available parametric equations. Based on the results of parametric FE study, a sample database was prepared for the DoB values and density histograms were generated for respective samples based on the Freedman-Diaconis rule. Thirteen theoretical PDFs were fitted to the developed histograms and the maximum likelihood (ML) method was applied to evaluate the parameters of fitted PDFs. In each case, the Kolmogorov-Smirnov test was used to evaluate the goodness of fit. Finally, the Generalized Extreme Value model was proposed as the governing probability distribution function for the DoB. After substituting the values of estimated parameters, nine fully defined PDFs were presented for the DoB at the crown, toe, and heel positions of the central and outer braces in tubular KT-joints subjected to three types of IPB moment loading.

1. Introduction

Circular hollow section members, also called tubulars, are the primary structural components of jacket-type offshore platforms widely used for the oil/gas production. The intersection among tubulars, in which the prepared ends of branch members (braces) are welded onto the undisturbed surface of a main member (chord), is called a tubular joint (Fig. 1). As a result of the formation and propagation of cracks due to wave induced cyclic loads, tubular joints are susceptible to fatigue-induced damage during their service life.

The stress-life (S-N) approach that is based on the hot-spot stress (HSS) calculation is widely used to estimate the fatigue life of a tubular joint. However, the study of a large number of fatigue test results have shown that tubular joints of different geometry or loading type but with similar HSSs often exhibit significantly different numbers of cycles to failure [1]. Such differences are thought to be attributable to changes in crack growth rate that is dependent on the through-the-thickness stress distribution which can be characterized by the degree of bending (DoB) defined as the ratio of bending stress to total external stress.

Typical stress distribution through the chord wall of a tubular joint is depicted in Fig. 2. Since for a deep crack, the weld-toe stress concentration has a relatively little effect on the through-the-thickness stress field [2], the stress distribution across the wall thickness is usually assumed to be a linear combination of membrane and bending stresses. Hence, the DoB can be expressed as:

$$\mathrm{DoB} = \frac{\sigma_B}{\sigma_T} = \frac{\sigma_B}{\sigma_B + \sigma_M} \tag{1}$$

where σ_T is the total stress; and σ_B and σ_M are the bending and membrane stress components, respectively.

The DoB value along the weld toe of a tubular joint, under any specific loading condition, is mainly determined by the joint geometry. To study the behavior of a tubular joint and to easily relate this behavior to the geometrical characteristics of the joint,

a set of dimensionless geometrical parameters has been defined. Fig. 1 depicts a tubular KT-joint with the geometrical parameters τ, γ, β, α, and α_B for chord and brace diameters: D and d, and their corresponding wall thicknesses: T and t, and lengths: L and l. Critical positions along the weld toe of central and outer braces for the calculation of the DoB values in a tubular joint, i.e. saddle, crown, toe, and heel have been shown in Fig. 1.

Since early 1990s, a number of research works has been devoted to the study of the DoB in simple tubular connections such as X- and K-joints. However, for tubular joints having more complex geometry such as KT-joints which are quite common in steel offshore structures, the DoB has not been comprehensively investigated.

Morgan and Lee [3] derived mean and design equations for DoB values at critical positions in axially loaded tubular K-joints. Design equations met all the acceptance criteria recommended by the UK DoE [4]. Chang and Dover [2] carried out a series of systematic thin-shell FE analyses for 330 tubular X- and DT-joints typically found in offshore structures under six different types of loading. A set of parametric equations was developed to calculate the DoB at critical positions. Lee and Bowness [5] proposed an engineering methodology for estimating stress intensity factor (SIF) solutions for semi-elliptical weld-toe cracks in tubular joints. The methodology uses the T-butt solutions proposed previously by the authors in conjunction with the stress concentration factors (SCFs) and the DoB values in uncracked tubular joints. Shen and Choo [6] determined the SIFs for a grouted tubular joint. They found that the fatigue strength of a grouted joint may be lower than that of as-welded joint, because when normalized with the HSS, the shape factor of grouted joint is higher than that of original as-welded joint due to the reduction in the DoB caused by the presence of in-filled grout in the chord. For grouted tubular joints, it is essential to consider the effect of the DoB in practical fatigue assessment using HSS approach. Ahmadi et al. [7] performed a set of parametric stress analyses on 81 K-joint FE models subjected to two different types of IPB loads. Analysis results were used to present general remarks on the effect of geometrical parameters on the DoB values at the toe and heel positions; and a new set of DoB parametric equations was developed. Ahmadi and Asoodeh [8] analyzed 81 K-joint FE models subjected to two types of out-of-plane bending (OPB) loading. Results were used to study the geometrical effects on the DoB at the saddle position; and two new DoB design formulas were proposed. Ahmadi and Asoodeh [9] studied the DoB in uniplanar tubular KT-joints of jacket structures subjected to axial loads. Their study was limited to the central brace DoB values and no design equation was proposed for the DoB along the weld toe of the outer braces. Also, IPB and OPB loadings were not included. Ahmadi and Amini Niaki [10] studied the degree of bending in two-planar tubular DT-joints under axial and bending loads. They developed a set of parametric equations to predict the DoB values at the saddle and crown positions.

In a deterministic fatigue analysis, limiting assumptions should be made on numerous input parameters some of which exhibit considerable scatter. Consequently, deterministic analyses usually result in conservative designs. This fact emphasizes the significance of reliability-based fatigue analysis and design methods in which the key parameters of the problem can be modeled as random variables. The fundamentals of fatigue reliability assessment, if properly applied, can provide immense insight into the fatigue performance and safety of the structural system. Regardless of the method used for the reliability-based fatigue analysis and design of offshore structures, the probabilistic and statistical measures of the DoB are required as input parameters. The DoB shows considerable scatter highlighting the significance of deriving its governing probability distribution function.

Ahmadi and Ghaffari [11] proposed a set of probability density functions for the DoB in tubular X-joints subjected to four types of bending loads including two types of IPB and two types of OPB moment loading. Ahmadi and Ghaffari [12] developed probability distribution models for the DoB and SIF values in axially-loaded tubular K-joints.

Based on the above discussion, it can be concluded that:

1. Despite the comprehensive research carried out on the study of SCFs and SIFs in tubular joints (e.g. [13-24] for SCFs, and [25, 26] for SIFs, among many others), the research works on the DoB in tubular joints are scarce and the studied joint types are limited to simple connections. Although tubular KT-joints are commonly found in steel offshore structures, the DoB in such joints has not been comprehensively investigated.
2. Results of research works reported in the literature are mostly suitable for deterministic analyses; and probabilistic studies are only limited to K- and X-joints. No probabilistic investigation has been carried out on the DoB of KT-joints; and there is no probability density function available for the DoB values to be used in reliability-based fatigue analysis and design of this type of joint.

In the present research, initially, available literature on the DoB was surveyed (Sect. 2). Afterwards, a total of 243 finite element (FE) analyses were carried out on 81 FE models of tubular KT-joints which are among the most common joint types in jacket-type oil/gas production platforms. FE analyses were conducted under three types of in-plane bending (IPB) loads as shown in Fig. 3. Generated FE models were validated

using the existing experimental data, FE results, and parametric equations. Based on a parametric FE investigation, a sample database was created for the DoB (Sect. 3); and density histograms were generated for respective samples (Sect. 4). Thirteen theoretical PDFs were fitted to the developed histograms and the maximum likelihood (ML) method was applied to evaluate the parameters of fitted PDFs (Sect. 5). In each case, the Kolmogorov-Smirnov test was used to assess the goodness of fit (Sect. 6). Finally, a probability distribution model was proposed for the DoB; and after substituting the values of estimated parameters, nine fully defined PDFs were presented for the DoB at the crown, toe, and heel positions of central and outer braces in tubular KT-joints subjected to three types of IPB moment loading (Sect. 7).

2. Preparation of the DoB sample database

2.1. FE modeling procedure

In the present research, FE-based software package ANSYS Ver. 11 was used for the FE modeling and analysis of tubular KT-joints subjected to IPB loadings in order to extract the DoB values for the probabilistic study. This section presents the details of FE modeling and analysis.

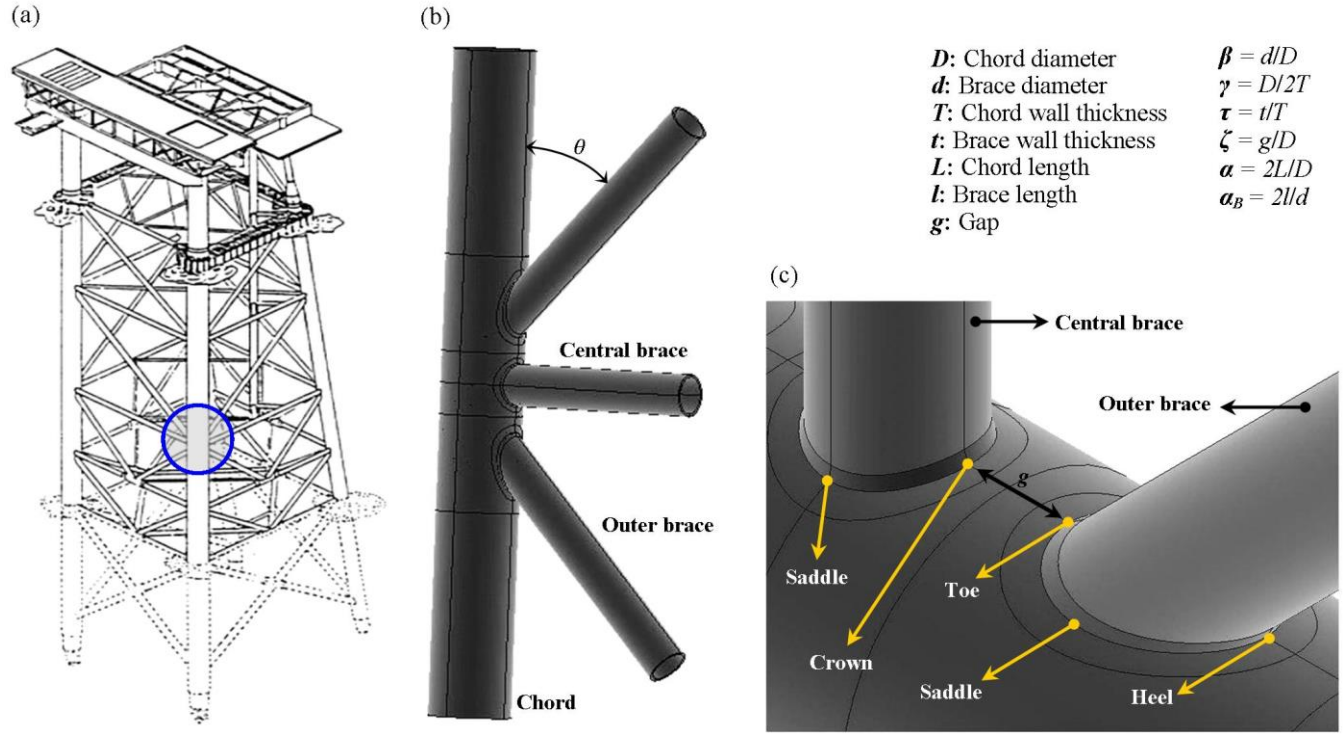

Fig. 1. (a) A tubular KT-joint in a typical offshore jacket structure, (b) Geometrical notation for a tubular KT-joint, (c) Critical positions along the weld toe of central and outer braces.

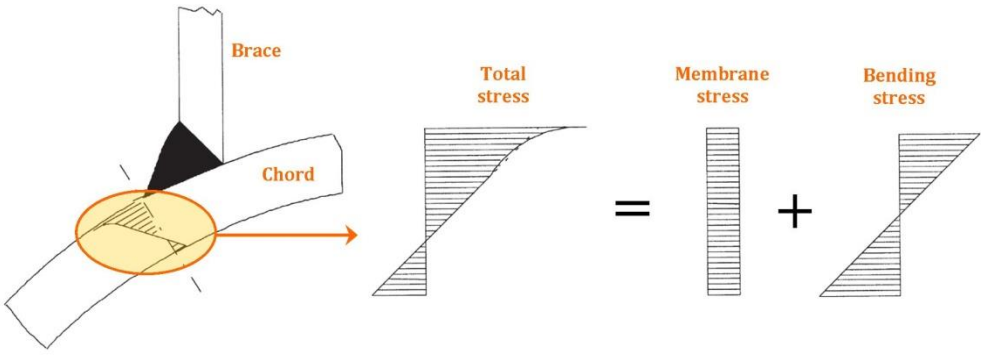

Fig. 2. Through-the-thickness stress distribution in a tubular joint.

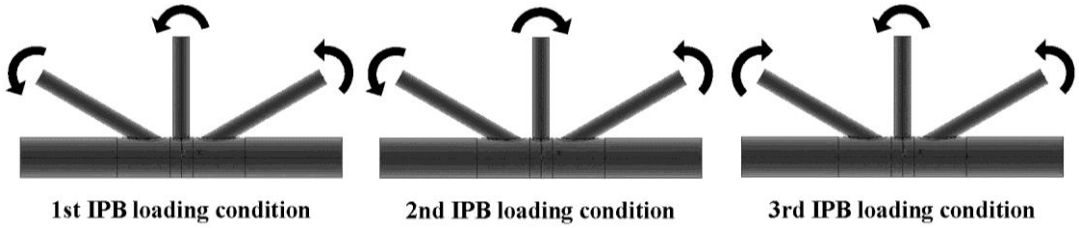

Fig. 3. Three applied IPB moment loading conditions.

2.1.1. Modeling of the weld profile

Accurate modeling of the weld profile is one of the important factors affecting the accuracy of the DoB results. In the present research, the welding size along the brace-to-chord intersection satisfies the AWS D 1.1 [27] specifications. The weld sizes at the crown, saddle, toe, and heel positions can be determined as follows:

$$H_w(\text{mm}) = 0.85t(\text{mm}) + 4.24$$

$$L_w = \frac{t}{2}\left[\frac{135^\circ - \psi\ (\text{deg.})}{45^\circ}\right]$$

$$\psi = \begin{cases} 90^\circ & \text{Crown} \\ 180^\circ - \cos^{-1}\beta\ (\text{deg.}) & \text{Saddle} \\ 180^\circ - \theta\ (\text{deg.}) & \text{Toe} \\ \theta\ (\text{deg.}) & \text{Heel} \end{cases} \quad (2)$$

The parameters of Eq. (2) are defined in Fig. 4. As an example, the weld profiles generated for the central and outer braces of the joint model SKTJ1 (α = 16, α_B = 8, ζ = 0.3, τ = 0.4, β = 0.4, γ = 12, θ = 30˚) are shown in Fig. 5. For details of the weld profile modeling according to AWS D 1.1 [27], the reader is referred to Lie et al. [28] and Ahmadi et al. [29].

2.1.2. Definition of boundary conditions

In view of the fact that the effect of chord end restraints is only significant for joints with α < 8 and high β and γ values, which do not commonly occur in practice [3, 30, 31], both chord ends were assumed to be fixed, with the corresponding nodes restrained.

Under each of the three considered loading conditions, only an appropriate portion of the entire tubular KT-joint is required to be modeled. The reason is the symmetry in geometry, material properties, and chord-end boundary conditions of the joint, as well as loading symmetry/antisymmetry. This allowed us to consider a reduced FE problem instead of the actual one. Thus, the order of the global stiffness matrix and total number of stiffness equations were reduced and computer solution time was substantially decreased. Table 1 and Fig. 6 describe the required portion to be modeled for each load case. Appropriate symmetric/antisymmetric boundary conditions were defined for the nodes located on the symmetry/antisymmetry planes.

2.1.3. Generation of the FE mesh

ANSYS element type SOLID95 was used in the present research to model the chord, braces, and the weld profiles. Using this type of 3-D brick elements, the weld profile can be modeled as a sharp notch. This method will produce more accurate and detailed stress distribution near the intersection in comparison with a shell analysis. The mesh generated for a tubular KT-joint is shown in Fig. 7.

2.1.4. Analysis procedure and extraction of DoB values

To calculate the DoB values in a tubular joint, static analysis of the linearly elastic type is suitable. The Young's modulus and Poisson's ratio were taken to be 207 GPa and 0.3, respectively.

In order to determine the weld-toe DoB values, according to Eq. (1), bending and membrane stress components should be known. These components can be calculated as follows:

$$\sigma_B = \frac{\sigma_O - \sigma_I}{2} \quad (3)$$

$$\sigma_M = \frac{\sigma_O + \sigma_I}{2} \quad (4)$$

where σ_o and σ_I are the hot-spot stresses (HSSs) at the weld toe on the outer and inner surfaces of the chord, respectively.

Eqs. (1), (3), and (4) lead to the following relation for the DoB based on the HSSs:

$$\text{DoB} = \frac{1}{2}\left(1 - \frac{\sigma_I}{\sigma_O}\right) \quad (5)$$

To determine the HSSs, the stress at the weld-toe position should be extracted from the stress field outside the region influenced by the local weld-toe geometry. The location from which the stresses have to be extrapolated, called extrapolation region, depends on the dimensions of the joint and on the position along the intersection. According to the recommendations of IIW-XV-E [32], the first extrapolation point should be at a distance of 0.4T from the weld toe, and the second point must be 1.0T further from the first point (Fig. 8a). The HSS is obtained by the linear extrapolation of the geometric stresses at these two points to the weld toe.

To extract and extrapolate the stresses perpendicular to the weld toe, as shown in Fig. 8a, the region between the weld toe and the second extrapolation point was meshed in such a way that each extrapolation point was placed between two nodes located in its immediate vicinity. These nodes are located on the element-generated lines which are perpendicular to the weld toe ($X_\perp$ direction in Fig. 8b).

2.1.5. Verification of the FE modeling

As far as the authors can tell, there is no experimental data available in the literature on the DoB values in tubular KT-joints. However, previous research works offer some experimental data, FE results, and parametric equations that can be used to validate the FE model developed in the present study.

2.1.5.a. Comparison with experimental data for the HSS

According to Eq. (5), DoB is a function of σ_o and σ_I that are the HSSs at the weld toe on the outer and

inner surfaces of the chord, respectively. Hence, if the proposed FE model could predict the HSS accurately, then undoubtedly it is capable of resulting in accurate DoB values.

To verify the developed FE modeling procedure, a validation FE model was generated and its results were compared with the results of experimental tests carried out by the first author on a KT-joint (Figs. 9 and 10). Details of the test setup and program presented by Ahmadi [33] are not repeated here for the sake of brevity.

Results of verification process are presented in Table 2. It can be seen that there is a good agreement between the results of present FE model and experimental data; and the average difference is about 10%. Hence, developed FE model can be considered to be accurate enough to provide valid results.

2.1.5.b. Comparison with available DoB parametric equations and FE results

A set of FE parametric studies have been conducted by Morgan and Lee [3], Ahmadi et al. [7], and Ahmadi and Asoodeh [8] for the prediction of DoB values in tubular K-joints under the axial, IPB, and OPB loadings, respectively. Results of these studies were used in the present research to validate the developed FE model. In order to do so, three K-joint FE models were generated having typical geometrical characteristics (Table 3) and they were analyzed under the axial, IPB, and OPB loadings shown in Fig. 11. Geometrical properties of the axially-loaded FE model were selected based on the data provided by HSE OTH 354 [34] for a steel specimen tested to determine the SCFs; and geometrical properties of the IPB- and OPB-loaded FE models were selected in accordance with the validity range of the FE study conducted by Ahmadi et al. [7] and Ahmadi and Asoodeh [8].

The method of geometrical modeling (introducing the chord, braces, and weld profiles), the mesh generation procedure (including the selection of element type and size), analysis method, and the method of DoB extraction are identical for the validating models and the KT-joint models used for the parametric study. Hence, the verification of DoB values derived from validating FE models with the results of equations proposed by Morgan and Lee [3], FE results of Ahmadi et al. [7], and FE results of Ahmadi and Asoodeh [8] lends some support to the validity of DoB values derived from the KT-joint FE models.

Results of verification process are presented in Table 4. It can be seen that there is a good agreement among the results of present FE model and equations proposed by Morgan and Lee [3], FE results of Ahmadi et al. [7], and FE results of Ahmadi and Asoodeh [8]. The average difference is less than 10%. Hence, generated FE models can be considered to be accurate enough to provide valid results.

2.2. Details of parametric study

Altogether, 243 stress analyses were carried out on 81 FE models using ANSYS Ver. 11 to investigate the effects of dimensionless geometrical parameters on the DoB values at the crown, toe, and heel positions in tubular KT-joints subjected to three different types of IPB moment loading (Fig. 3).

Different values assigned to the parameters β, γ, τ, and θ have been presented in Table 5. These values cover the practical ranges of the dimensionless parameters typically found in tubular joints of offshore jacket structures.

Where the gap between the braces is not very large, the relative gap ($\zeta = g / D$) has no considerable effect on the stress and strain distribution. The validity range for this statement is $0.2 \leq \zeta \leq 0.6$ [19]. Hence, a typical value of $\zeta = 0.3$ was designated for all joints. Sufficiently long chord greater than six chord diameters (i.e. $\alpha \geq 12$) should be used to ensure that the stresses at the brace/chord intersection are not affected by the chord's boundary conditions [13]. The brace length has no effect on the HSSs when the parameter α_B is greater than a critical value [16]. According to Chang and Dover [35], this critical value is about 6. In the present study, in order to avoid the effect of short brace length, a realistic value of $\alpha_B = 8$ was selected for all joints.

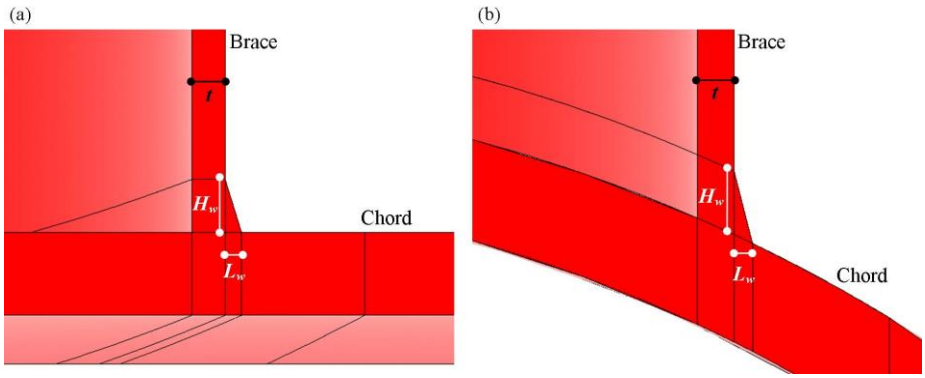

Fig. 4. Weld dimensions: (a) Crown position, (b) Saddle position.

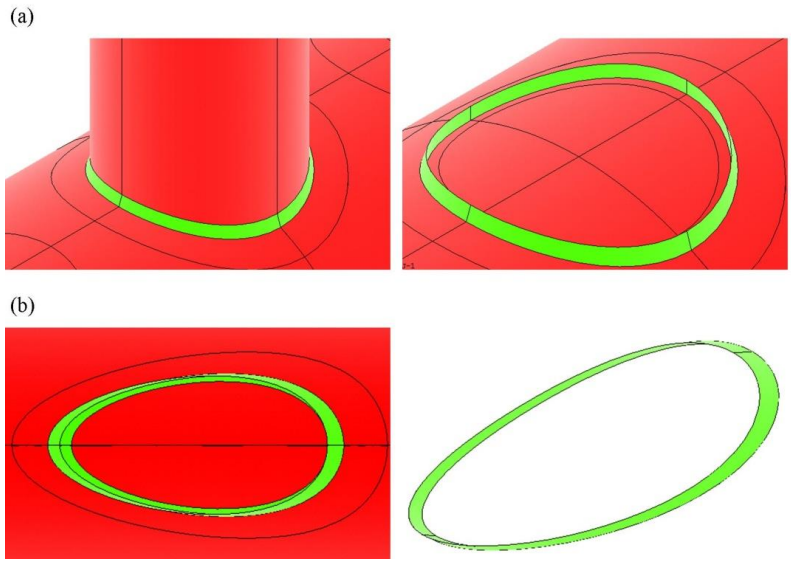

Fig. 5. Simulated weld profile: (a) Central brace, (b) Outer brace.

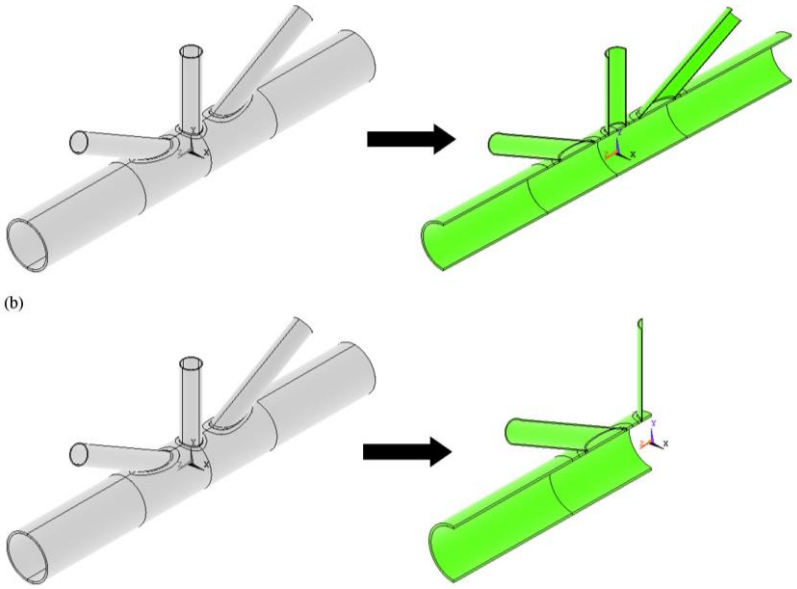

Fig. 6. Appropriate portion of the entire tubular KT-joint required to be modeled for each load case based on Table 1: (a) ½, (b) ¼.

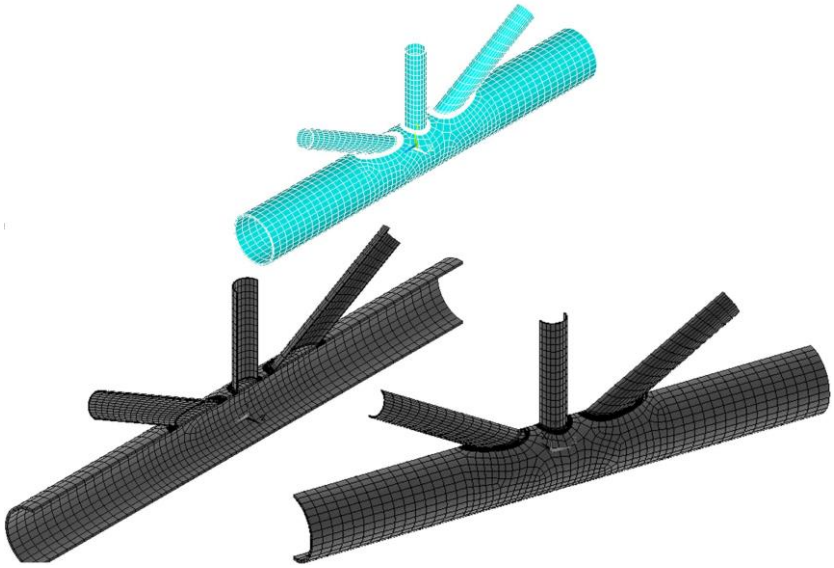

Fig. 7. Generated mesh for a tubular KT-joint using the sub-zone method.

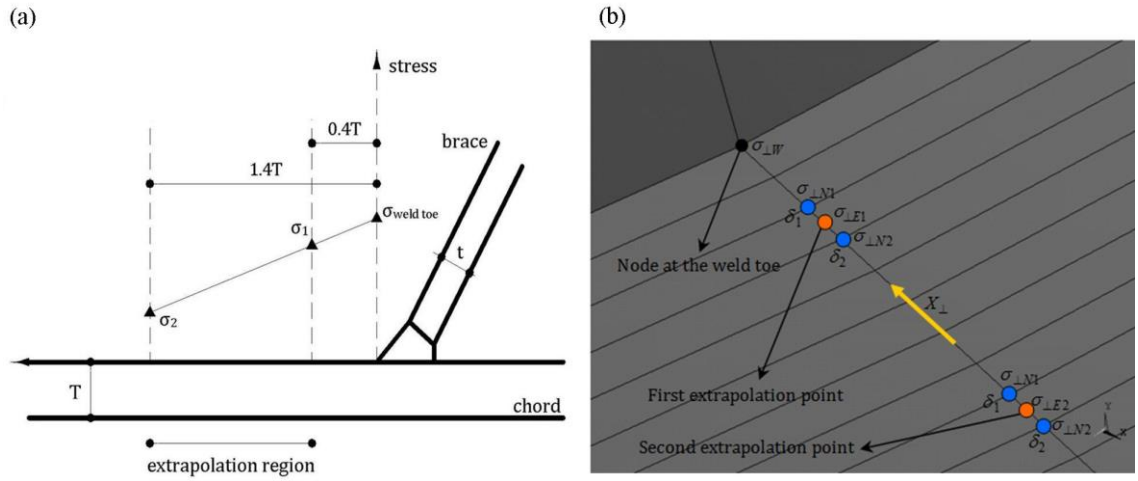

Fig. 8. (a) Extrapolation method recommended by IIW-XV-E [32], (b) Interpolations and extrapolations necessary to compute the DoB value based on the HSSs at the weld toe.

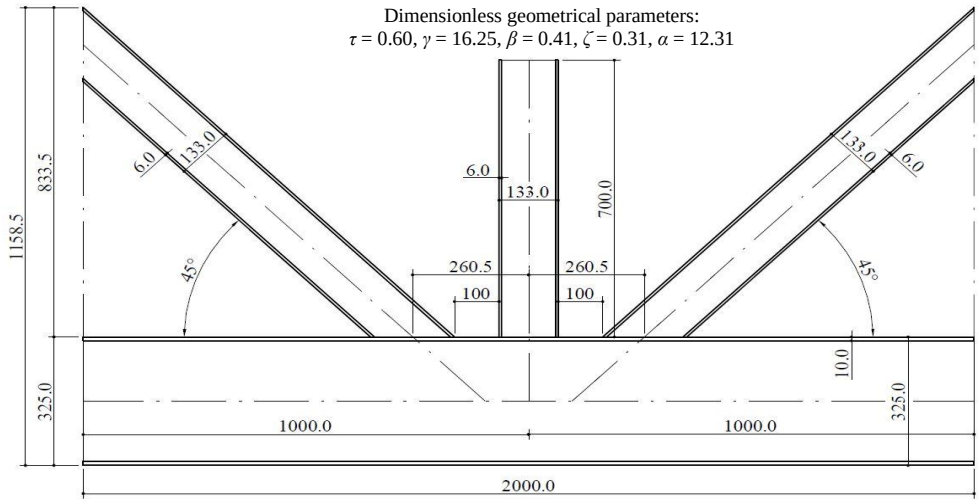

Fig. 9. Geometrical characteristics of tested tubular KT-joint specimen (unit: mm) [33].

Fig. 10. Test setup [33]: (a) View of the test rig and KT-joint specimen, (b) Strain gauges attached along the brace-to-chord intersection, (c) Connecting the strain gauges to the data logger.

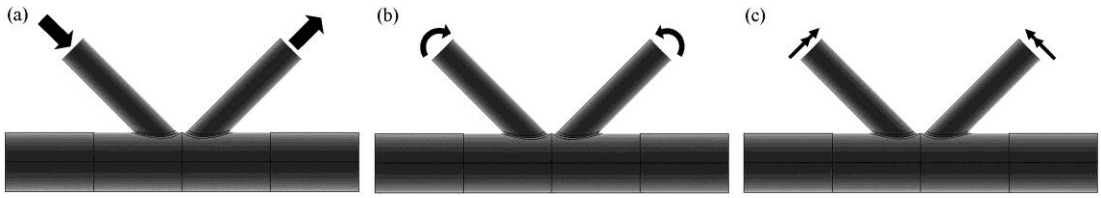

Fig. 11. Load cases for FE model validation: (a) Balanced axial loading studied by Morgan and Lee [3], (b) Balanced IPB loading studied by Ahmadi et al. [7], (c) Balanced OPB loading studied by Ahmadi and Asoodeh [8].

The 81 generated models span the following ranges of geometrical parameters:

$$\begin{aligned} &0.4 \le \beta \le 0.6 \\ &12 \le \gamma \le 24 \\ &0.4 \le \tau \le 1.0 \\ &30^\circ \le \theta \le 60^\circ \end{aligned} \quad (6)$$

2.3. Organization of the DoB samples

The DoB values extracted from the results of 243 FE analyses were organized as nine samples for further statistical and probabilistic analyses. Samples 1−3 included the DoB values at the crown position of the central brace under the 1st–3rd IPB loading conditions, respectively; while samples 4−6 included the DoB values at the toe position of the outer brace under the 1st–3rd IPB loading conditions, respectively; and samples 7−9 included the DoB values at the heel position of the outer brace under the 1st–3rd IPB loading conditions, respectively. Values of the size (n), mean (μ), standard deviation (σ), coefficient of skewness (α_3), and coefficient of kurtosis (α_4) for Samples 1−3 are listed in Table 6 as an example.

The value of α_3 for the crown and heel position DoB samples is positive which means that the probability distribution for these samples is expected to have a longer tail on the right, which is toward increasing values, than on the left. However, the value of α_3 for the toe position DoB samples is negative which means that the probability distribution for these samples is expected to have a longer tail on the left, which is toward decreasing values, than on the right.

Moreover, the value of α_4 for the crown and toe position DoB samples is smaller than three meaning that the probability distribution is expected to be mild-peak (platykurtic) for these samples; while the value of α_4 for the heel position DoB samples is greater than three which means that for these samples, the probability distribution is expected to be sharp-peak (leptokurtic).

3. Probabilistic analysis

3.1. Generation of density histograms based on the Freedman-Diaconis rule

To generate a density histogram, the range of data (R) is divided into a number of classes and the number of occurrences in each class is counted and tabulated. These are called frequencies. Then, the relative frequency of each class can be obtained through dividing its frequency by the sample size. Afterwards, the density is calculated for each class through dividing the relative frequency by the class width. The width of classes is usually made equal to facilitate interpretation. One of the widely accepted rules to determine the number of classes is the Freedman-Diaconis rule [36].

As an example, density histograms of Samples 1−6 are shown in Fig. 12. This figure shows that, as it was expected from the values of α_3 and α_4:

1. The right tail is longer than the left one in the histograms of samples 1−3 and 7−9; while in the histograms of samples 4−6, the left tail is longer.
2. The histograms of samples 1−6 are platykurtic; while the histograms of samples 7−9 are leptokurtic.

3.2. Application of the maximum likelihood method for PDF fitting

Thirteen different PDFs were fitted to the density histograms to assess the degree of fitting of various distributions to the DoB samples. In each case, distribution parameters were estimated using the maximum likelihood (ML) method. Results for Samples 1−3 are given in Table 7 as an example. For more information regarding the definition of distribution parameters, the reader is referred to Kottegoda and Rosso [36].

3.3. Assessment of the goodness-of-fit based on the Kolmogorov-Smirnov test

The Kolmogorov-Smirnov goodness-of-fit test is a nonparametric test that relates to the cumulative distribution function (CDF) of a continuous variable. The test statistic (d_n), in a two-sided test, is the maximum absolute difference (which is usually the vertical distance) between the empirical and hypothetical CDFs.

A large value of this statistic indicates a poor fit. Hence, acceptable values should be known. The critical values $D_{n,\xi}$ for large samples, say $n > 35$, are $(1.3581/\sqrt{n})$ and $(1.6276/\sqrt{n})$ for $\xi = 0.05$ and 0.01, respectively [36] where ξ is the significance level.

As an example, empirical distribution functions for Samples 1–6 have been shown in Fig. 13.

Theoretical continuous CDFs fitted to the empirical distribution functions of Samples 4–9 have been shown in Fig. 14 as an example.

Results of the Kolmogorov-Smirnov test for Sample 1 are given in Table 8 as an example. The Beta,

Lognormal, and Log-logistic distributions had the smallest d_n value for samples 1−3, respectively. The Extreme Value distribution has the smallest d_n for samples 4 and 6; and Generalized Extreme Value distribution has the smallest d_n for samples 5 and 7−9. Hence, they are the best-fitted distributions for the corresponding DoB samples (Fig. 15).

3.4. Proposed probability distribution model for the DoB

The best fitted distributions for the generated DoB samples were introduced in Sect. 6. According to the results of the Kolmogorov-Smirnov test, it can be seen that the best-fitted distributions for the nine studied samples include five different models: Beta, Lognormal, Log-logistic, Extreme Value, and Generalized Extreme Value distributions. The diversity of the best-fitted probability models derived for the studied DoB values may practically result in the confusion and difficulty of their application for the fatigue reliability analysis and design. Hence, reducing the number of distribution types proposed for the DoB values might be a good idea. In order to do so, the top three distribution functions for each DoB sample were identified (Table 9 for Samples 1–3 as an example). The aim was to propose a single probability model to cover all the DoB samples. It should be noted that, for each sample, all of the three mentioned functions have acceptable fit according to the Kolmogorov-Smirnov test.

After surveying the data (presented in Table 9 for Samples 1–3 as an example), the Generalized Extreme Value model is proposed as the governing probability distribution function for the DoB values. The difference between the test statistics of the proposed distribution and the best-fitted one for each sample is presented in Tables 10–12. Using the information presented in these tables, the analyst is able to make a choice, based on the engineering judgment, between the best-fitted and the proposed probability models for each of the studied cases.

The PDF of the Generalized Extreme Value distribution is expressed as [36]:

$$f_X(x) = \left(\frac{1}{\sigma}\right)\exp\left(-\left(1+k\,\frac{(x-\mu)}{\sigma}\right)^{-\frac{1}{k}}\right) \times\left(1+k\,\frac{(x-\mu)}{\sigma}\right)^{-1-\frac{1}{k}} \tag{7}$$

After substituting the values of estimated parameters (for example, from Table 7 for Samples 1–3), following probability density functions are proposed for the DoB values in tubular KT-joints subjected to the three considered IPB load cases defined in Fig. 3:

Crown position of the central brace−1st IPB loading condition:

$$f_X(x) = 36.27144\exp\left[-\left(1-10.35238\,(x-0.87975)\right)^{3.50368}\right]\left[1-10.35238\,(x-0.87975)\right]^{2.50368} \tag{8}$$

Crown position of the central brace−2nd IPB loading condition:

$$f_X(x) = 25.83359\exp\left[-\left(1-7.70786\,(x-0.67778)\right)^{3.35159}\right]\left[1-7.70786\,(x-0.67778)\right]^{2.35159} \tag{9}$$

Crown position of the central brace−3rd IPB loading condition:

$$f_X(x) = 21.33752\exp\left[-\left(1-1.64464\,(x-0.56854)\right)^{12.97399}\right]\left[1-1.64464\,(x-0.56854)\right]^{11.97399} \tag{10}$$

Toe position of the outer brace−1st IPB loading condition:

$$f_X(x) = 21.14500\exp\left[-\left(1-10.90587\,(x-0.78212)\right)^{1.93886}\right]\left[1-10.90587\,(x-0.78212)\right]^{0.93886} \tag{11}$$

Toe position of the outer brace−2nd IPB loading condition:

$$f_X(x) = 14.84726\exp\left[-\left(1-9.23936\,(x-0.68232)\right)^{1.60696}\right]\left[1-9.23936\,(x-0.68232)\right]^{0.60696} \tag{12}$$

Toe position of the outer brace−3rd IPB loading condition:

$$f_X(x) = 14.08514\exp\left[-\left(1-7.90137\,(x-0.64752)\right)^{1.78262}\right]\left[1-7.90137\,(x-0.64752)\right]^{0.78262} \tag{13}$$

Heel position of the outer brace−1st IPB loading condition:

$$f_X(x) = 18.68925\exp\left[-\left(1+2.92638\,(x-0.76812)\right)^{-6.38647}\right]\left[1+2.92638\,(x-0.76812)\right]^{-7.38647} \tag{14}$$

Heel position of the outer brace−2nd IPB loading condition:

$$f_X(x) = 15.50727\exp\left[-\left(1-0.17675\,(x-0.79780)\right)^{87.73700}\right]\left[1-0.17675\,(x-0.79780)\right]^{86.73700} \tag{15}$$

Heel position of the outer brace−3rd IPB loading condition:

$$f_X(x) = 17.14981\exp\left[-\left(1+2.11756\,(x-0.82963)\right)^{-8.09887}\right]\left[1+2.11756\,(x-0.82963)\right]^{-9.09887} \tag{16}$$

where X denotes the DoB as a random variable and x represents its values.
Developed PDFs are shown in Fig. 16 for Samples 1–6 as an example.

4. Conclusions

In the present paper, a total of 243 FE analyses were carried out on 81 models of KT-joints subjected to three types of IPB moment loading. Generated FE models were validated using experimental data, previous FE results, and available parametric equations. FE analysis results were used to develop a set of PDFs for the DoB in IPB-loaded KT-joints. Based on the results of parametric FE study, a sample database was prepared for the DoB values and density histograms were generated for respective samples based on the Freedman-Diaconis rule. Thirteen theoretical PDFs were fitted to the developed histograms and the ML method was applied to evaluate the parameters of fitted PDFs. In each case, the Kolmogorov-Smirnov test was used to evaluate the goodness of fit. Finally, the Generalized Extreme Value model was proposed as the governing probability distribution function for the DoB. After substituting the values of estimated parameters, nine fully defined PDFs were presented for the DoB at the crown, toe, and heel positions of central and outer braces in tubular KT-joints subjected to three types of IPB moment loading.

Acknowledgments

Useful comments of anonymous reviewers on draft version of this paper are highly appreciated.

References

1- Connolly, M.P.M., (1986), *A fracture mechanics approach to the fatigue assessment of tubular welded Y and K-joints*, PhD Thesis, University College London, UK.
2- Chang, E., Dover, W.D., (1999), *Prediction of degree of bending in tubular X and DT joints*, International Journal of Fatigue, Vol. 21 (2), p. 147-161.
3- Morgan, M.R., Lee, M.M.K., (1998), *Prediction of stress concentrations and degrees of bending in axially loaded tubular K-joints*, Journal of Constructional Steel Research, Vol. 45 (1), p. 67-97.
4- UK Department of Energy (DoE), (1995), *Background to new fatigue design guidance for steel joints and connections in offshore structures*, London, UK.
5- Lee, M.M.K., Bowness, D., (2002), *Estimation of stress intensity factor solutions for weld toe cracks in offshore tubular joints*, International Journal of Fatigue, Vol. 24, p. 861-875.
6- Shen, W., Choo, Y.S., (2012), *Stress intensity factor for a tubular T-joint with grouted chord*, Engineering Structures, Vol. 35, p. 37-47.
7- Ahmadi, H., Lotfollahi-Yaghin, M.A., Asoodeh, S., (2015), *Degree of bending (DoB) in tubular K-joints of offshore structures subjected to in-plane bending (IPB) loads: Study of geometrical effects and parametric formulation*, Ocean Engineering, Vol. 102, p. 105-116.
8- Ahmadi, H., Asoodeh, S., (2016), *Parametric study of geometrical effects on the degree of bending (DoB) in offshore tubular K-joints under out-of-plane bending loads*, Applied Ocean Research, Vol. 58, p. 1-10.
9- Ahmadi, H., Asoodeh, S, (2015), *Degree of bending (DoB) in tubular KT-joints of jacket structures subjected to axial loads*, International Journal of Maritime Technology, Vol. 4 (2), p. 65-75.
10- Ahmadi, H., Amini Niaki, M., (2019), *Effects of geometrical parameters on the degree of bending (DoB) in two-planar tubular DT-joints of offshore jacket structures subjected to axial and bending loads*, Marine Structures, Vol. 64 (C), p. 229-245.
11- Ahmadi, H., Ghaffari, A.R., (2015), *Probabilistic assessment of degree of bending (DoB) in tubular X-joints of offshore structures subjected to bending loads*, Advances in Civil Engineering, p. 1-12.
12- Ahmadi, H., Ghaffari, A.R., (2015), *Probabilistic analysis of stress intensity factor (SIF) and degree of bending (DoB) in axially loaded tubular K-joints of offshore structures*, Latin American Journal of Solids and Structures, Vol. 12 (11), p. 2025-2044.
13- Efthymiou, M., (1988), *Development of SCF formulae and generalized influence functions for use in fatigue analysis*, OTJ 88, Surrey, UK.
14- Hellier, A.K., Connolly, M., Dover, W.D., (1990), *Stress concentration factors for tubular Y and T-joints*, International Journal of Fatigue, Vol. 12, p. 13-23.
15- Morgan, M.R., Lee, M.M.K., (1998), *Parametric equations for distributions of stress concentration factors in tubular K-joints under out-of-plane moment loading*, International Journal of Fatigue, Vol. 20, 449-461.
16- Chang, E., Dover, W.D., (1999), *Parametric equations to predict stress distributions along the intersection of tubular X and DT-joints*. International Journal of Fatigue, Vol. 21, p. 619-635.
17- Shao, Y.B., (2007), *Geometrical effect on the stress distribution along weld toe for tubular T- and K-joints under axial loading*, Journal of Constructional Steel Research, Vol. 63, p. 1351-1360.
18- Shao, Y.B., Du, Z.F., Lie, S.T., (2009), *Prediction of hot spot stress distribution for tubular K-joints under basic loadings*, Journal of Constructional Steel Research, Vol. 65, 2011-2026.
19- Lotfollahi-Yaghin, M.A., Ahmadi, H., (2010), *Effect of geometrical parameters on SCF distribution along the weld toe of tubular KT-joints under balanced axial loads*, International Journal of Fatigue, Vol. 32, p. 703-719.

20- Ahmadi, H., Lotfollahi-Yaghin, M.A., Aminfar, M.H., (2011), *Geometrical effect on SCF distribution in uni-planar tubular DKT-joints under axial loads*, Journal of Constructional Steel Research, Vol. 67, p. 1282-1291.

21- Lotfollahi-Yaghin, M.A., Ahmadi, H., (2011), *Geometric stress distribution along the weld toe of the outer brace in two-planar tubular DKT-joints: parametric study and deriving the SCF design equations*, Marine Structures, Vol. 24, p. 239-260.

22- Ahmadi, H., Lotfollahi-Yaghin, M.A., (2012), *Geometrically parametric study of central brace SCFs in offshore three-planar tubular KT-joints*, Journal of Constructional Steel Research, Vol. 71, 149-161.

23- Ahmadi, H., Lotfollahi-Yaghin, M.A., Shao, Y.B., (2013), *Chord-side SCF distribution of central brace in internally ring-stiffened tubular KT-joints: A geometrically parametric study*, Thin-Walled Structures, Vol. 70, p. 93-105.

24- Ahmadi, H., Zavvar, E., (2016), *The effect of multi-planarity on the SCFs in offshore tubular KT-joints subjected to in-plane and out-of-plane bending loads*, Thin-Walled Structures, Vol. 106, p. 148-165.

25- Shao, Y.B., Lie, S.T., (2005), *Parametric equation of stress intensity factor for tubular K-joint under balanced axial loads*, International Journal of Fatigue, Vol. 27, 666-679.

26- Shao, Y.B., (2006), *Analysis of stress intensity factor (SIF) for cracked tubular K-joints subjected to balanced axial load*, Engineering Failure Analysis, Vol. 13, p. 44-64.

27- American Welding Society (AWS), (2002), *Structural welding code: AWS D 1.1*, Miami (FL), US.

28- Lie, S.T., Lee, C.K., Wong, S.M., (2001), *Modeling and mesh generation of weld profile in tubular Y-joint*, Journal of Constructional Steel Research, Vol. 57, p. 547-567.

29- Ahmadi, H., Lotfollahi-Yaghin, M.A., Shao, Y.B., Aminfar M.H., (2012), *Parametric study and formulation of outer-brace geometric stress concentration factors in internally ring-stiffened tubular KT-joints of offshore structures*, Applied Ocean Research, Vol. 38, p. 74-91.

30- Wordsworth, A.C., Smedley, G.P., (1978), *Stress concentrations at unstiffened tubular joints*, Proceedings of the European Offshore Steels Research Seminar, Paper 31, Cambridge, UK.

31- Smedley, P., Fisher, P., (1991), *Stress concentration factors for simple tubular joints*, Proceedings of the International Offshore and Polar Engineering Conference (ISOPE), Edinburgh, p. 475-483.

32- IIW-XV-E, (1999), *Recommended fatigue design procedure for welded hollow section joints, IIW Docs, XV-1035-99/XIII-1804-99*, International Institute of Welding, France.

33- Ahmadi, H., (2012), *Experimental and numerical investigation of the SCF distribution in unstiffened and stiffened uniplanar tubular KT-joints of steel platforms and the extension of numerical study to multi-planar joints*, PhD Thesis, Faculty of Civil Engineering, University of Tabriz, Tabriz, Iran (In Farsi).

34- UK Health and Safety Executive, (1997), *OTH 354: Stress concentration factors for simple tubular joints- assessment of existing and development of new parametric formulae*. Prepared by Lloyd's Register of Shipping, UK.

35- Chang, E., Dover, W.D., (1996), *Stress concentration factor parametric equations for tubular X and DT joints*, International Journal of Fatigue, Vol. 18 (6), p. 363-387.

36- Kottegoda, N.T., Rosso, R., (2008), *Applied statistics for civil and environmental engineers*, 2nd Edition, Blackwell Publishing Ltd, UK.

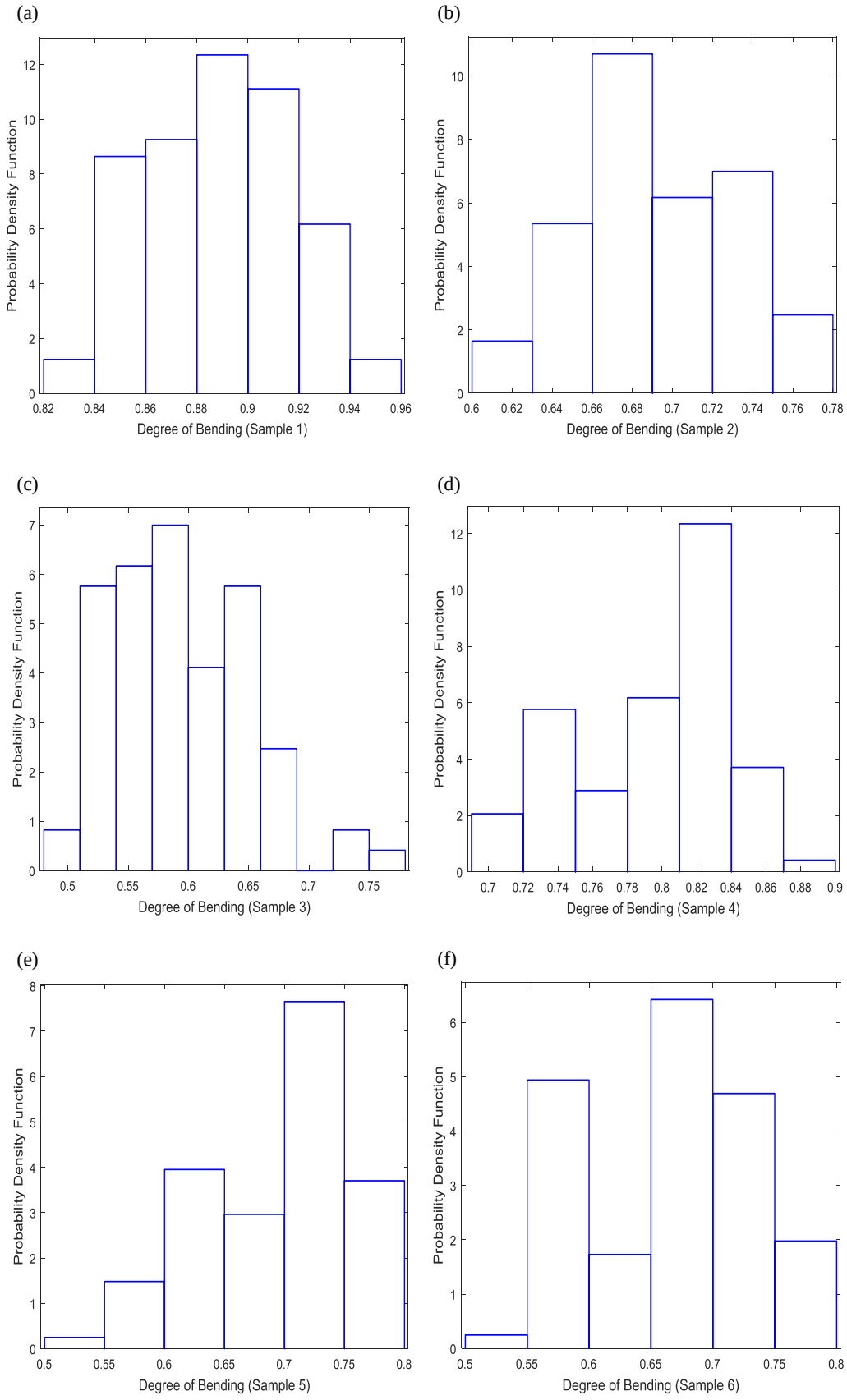

Fig. 12. Density histograms generated for the DoB samples: (a) Sample 1 (Cr, CB, 1st IPB LC), (b) Sample 2 (Cr, CB, 2nd IPB LC), (c) Sample 3 (Cr, CB, 3rd IPB LC), (d) Sample 4 (T, OB, 1st IPB LC), (e) Sample 5 (T, OB, 2nd IPB LC), (f) Sample 6 (T, OB, 3rd IPB LC) [Key– Cr: Crown; T: Toe; CB: Central brace; OB: Outer brace; LC: Loading condition].

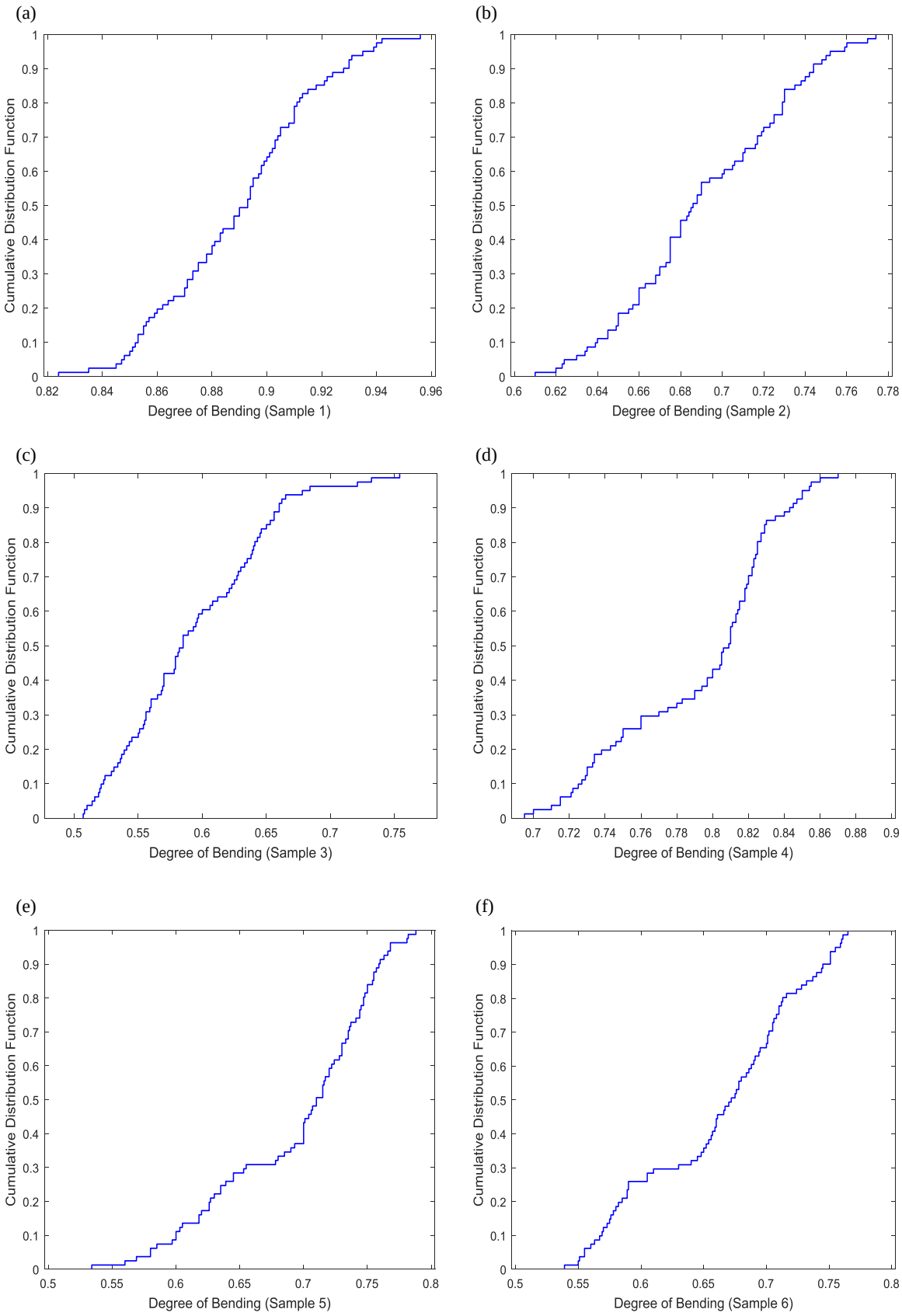

Fig. 13. Empirical cumulative distribution functions for generated DoB samples: (a) Sample 1 (Cr, CB, 1st IPB LC), (b) Sample 2 (Cr, CB, 2nd IPB LC), (c) Sample 3 (Cr, CB, 3rd IPB LC), (d) Sample 4 (T, OB, 1st IPB LC), (e) Sample 5 (T, OB, 2nd IPB LC), (f) Sample 6 (T, OB, 3rd IPB LC) [Key– Cr: Crown; T: Toe; CB: Central brace; OB: Outer brace; LC: Loading condition].

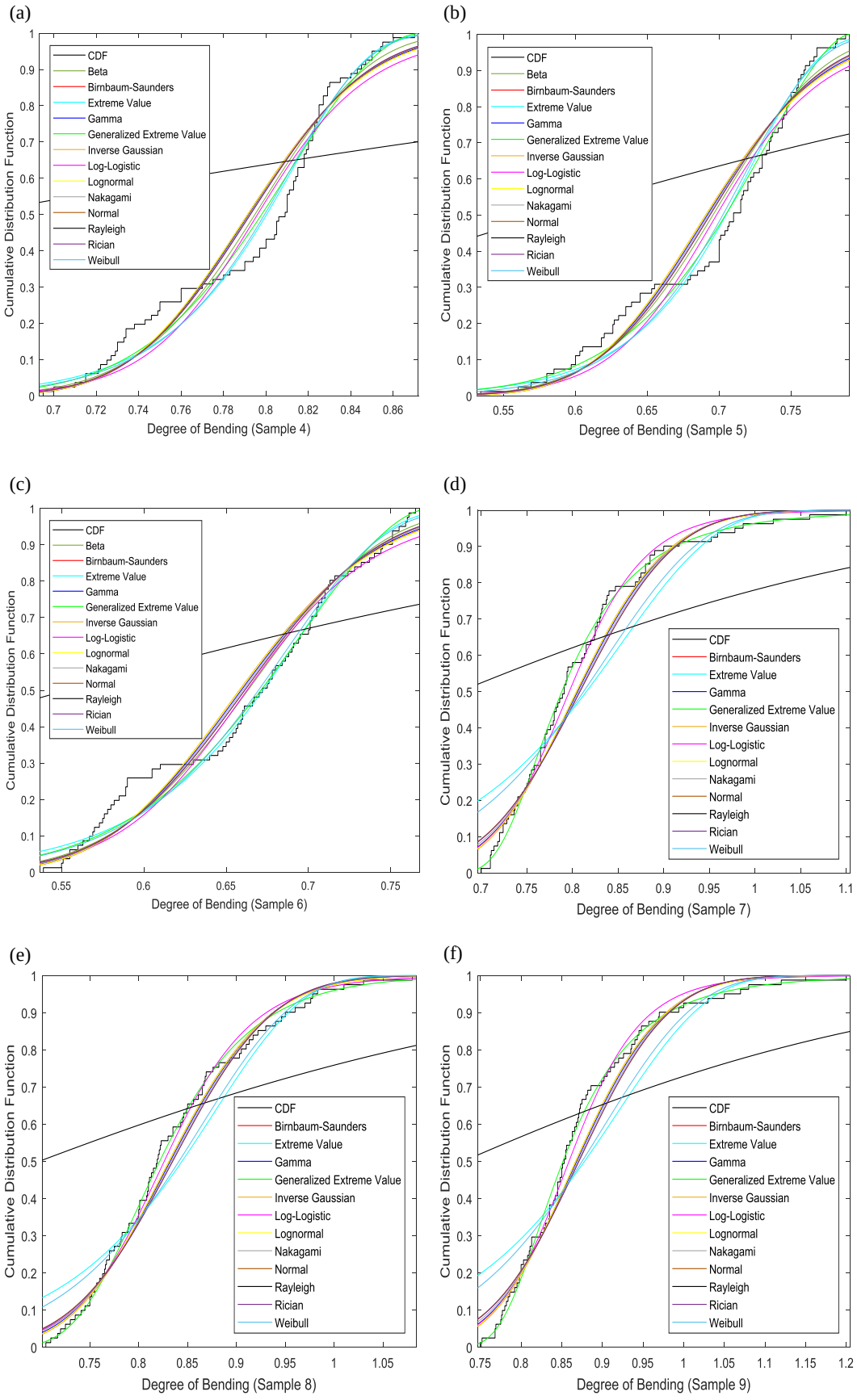

Fig. 14. Theoretical continuous CDFs fitted to the empirical CDFs of generated DoB samples: (a) Sample 1 (Cr, CB, 1st IPB LC), (b) Sample 2 (Cr, CB, 2nd IPB LC), (c) Sample 3 (Cr, CB, 3rd IPB LC), (d) Sample 4 (T, OB, 1st IPB LC), (e) Sample 5 (T, OB, 2nd IPB LC), (f) Sample 6 (T, OB, 3rd IPB LC) [Key– Cr: Crown; T: Toe; CB: Central brace; OB: Outer brace; LC: Loading condition].

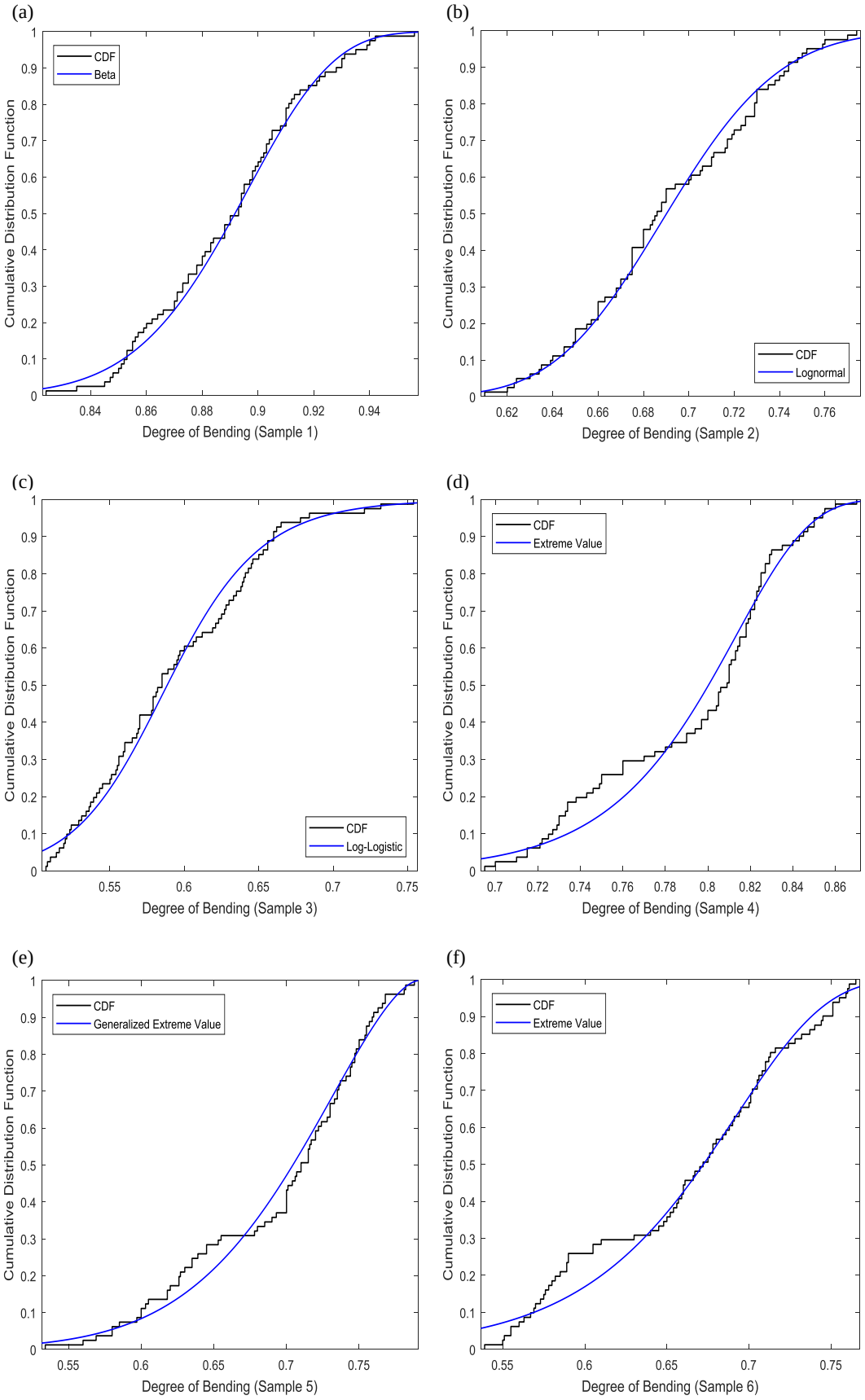

Fig. 15. The best-fitted distributions according to the Kolmogorov-Smirnov test: (a) Sample 1 (Cr, CB, 1st IPB LC), (b) Sample 2 (Cr, CB, 2nd IPB LC), (c) Sample 3 (Cr, CB, 3rd IPB LC), (d) Sample 4 (T, OB, 1st IPB LC), (e) Sample 5 (T, OB, 2nd IPB LC), (f) Sample 6 (T, OB, 3rd IPB LC) [Key– Cr: Crown; T: Toe; CB: Central brace; OB: Outer brace; LC: Loading condition].

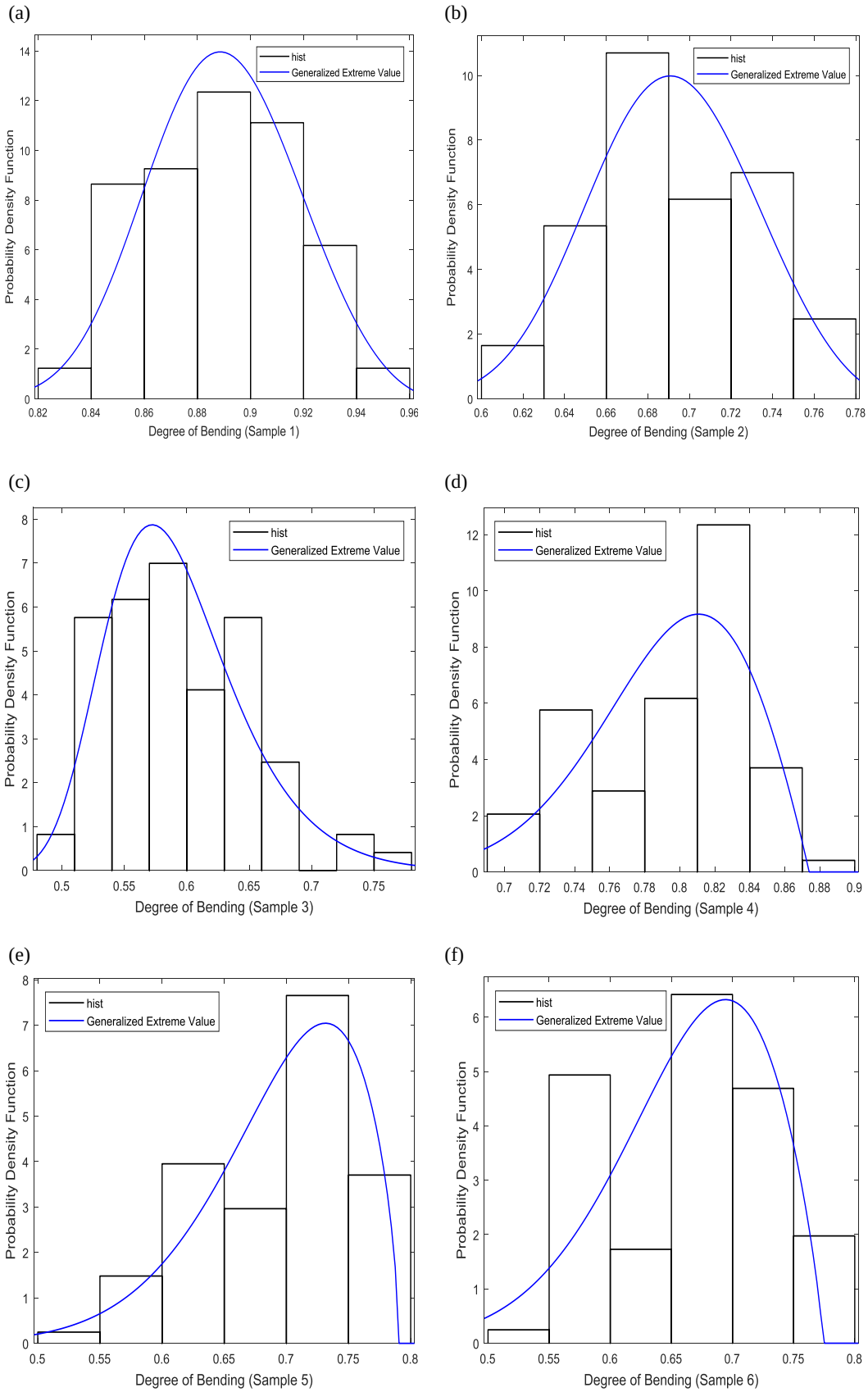

Fig. 16. Proposed PDFs for generated DoB samples: (a) Sample 1 (Cr, CB, 1st IPB LC), (b) Sample 2 (Cr, CB, 2nd IPB LC), (c) Sample 3 (Cr, CB, 3rd IPB LC), (d) Sample 4 (T, OB, 1st IPB LC), (e) Sample 5 (T, OB, 2nd IPB LC), (f) Sample 6 (T, OB, 3rd IPB LC) [Key– Cr: Crown; T: Toe; CB: Central brace; OB: Outer brace; LC: Loading condition].

Table 1. Appropriate portion of an entire tubular KT-joint required to be modeled for each load case.

Load case (Fig. 3)	Required portion to be modeled
1st IPB moment loading condition	¼ (Fig. 6b)
2nd IPB moment loading condition	¼ (Fig. 6b)
3rd IPB moment loading condition	½ (Fig. 6a)

Table 2. Results of FE model verification based on experimental data.

Loading	Position	HSS value of the chord's outer surface σ_O (N/m^2)		Difference
		Present FE model	Experimental test [33]	
Axial	Saddle	5.48e+6	5.89e+6	6.96%
	Crown	2.94e+6	3.38e+6	13.02%

Table 3. Geometrical properties of the tubular K-joint specimen used for the verification of FE models.

Loading	Joint ID	D (mm)	τ	β	γ	α	θ	ζ
Axial	JISSP 3.3 [34]	508	1.0	0.5	20.3	12.6	45˚	0.15
IPB	KJ-1 [7]	500	0.4	0.4	12.0	12.0	30˚	0.15
OPB	KJ-1 [8]	500	0.4	0.4	12.0	12.0	30˚	0.15

Table 4. Results of the FE model verification based on available parametric equations/FE results.

Loading	Position	DoB values		Difference
		Present FE model	Available data	
Axial (Fig. 12a)	Saddle	0.6666	0.5529 (Morgan and Lee [3] Eq. (3d))	20.56%
	Toe	0.8727	0.8989 (Morgan and Lee [3] Eq. (3f))	2.91%
	Heel	0.7728	0.6997 (Morgan and Lee [3] Eq. (3b))	10.45%
IPB (Fig. 12b)	Toe	0.5991	0.5742 (Ahmadi et al. [7] FE model)	4.16%
OPB (Fig. 12c)	Saddle	0.8920	0.8045 (Ahmadi and Asoodeh [8] FE model)	10.87%

Table 5. Values assigned to each dimensionless parameter.

Parameter	Definition	Value(s)
β	d/D	0.4, 0.5, 0.6
γ	$D/2T$	12, 18, 24
τ	t/T	0.4, 0.7, 1.0
θ		30˚, 45˚, 60˚
ζ	g/D	0.3
α	$2L/D$	16
α_B	$2l/d$	8

Table 6. Statistical measures of generated DoB samples at the crown position of the central brace under IPB loadings.

Statistical measure	DoB samples		
	Sample 1	Sample 2	Sample 3
	1st IPB load case	2nd IPB load case	3rd IPB load case
n	81	81	81
μ	0.8895	0.6913	0.5926
σ	0.0279	0.0394	0.0552
α_3	0.0201	0.0788	0.5284
α_4	2.4055	2.1124	2.8107

Table 7. Estimated parameters for PDFs fitted to the density histograms of DoB samples at the crown position of the central brace under the IPB loadings.

Fitted PDF	Parameters	Estimated values		
		Sample 1	Sample 2	Sample 3
		1st IPB load case	2nd IPB load case	3rd IPB load case
Beta	a	106.262	95.1363	46.0466
	b	13.1971	42.4829	31.6323
Birnbaum-Saunders	β_0	0.889062	0.690177	0.590175
	γ_0	0.0311572	0.0566481	0.0911977
Extreme Value	μ	0.903347	0.710948	0.621296
	σ	0.0266994	0.0371451	0.0600721
Gamma	a	1031.04	312.152	119.434
	b	0.000862718	0.00221458	0.004962
Generalized Extreme Value	k	-0.285414	-0.298366	-0.0770773
	σ	0.0275699	0.0387093	0.0468658
	μ	0.879746	0.677775	0.568542
Inverse Gaussian	μ	0.889494	0.691284	0.59263
	λ	916.053	215.248	71.1072
Log-logistic	μ	-0.11727	-0.370982	-0.530274
	σ	0.0182218	0.0336679	0.0536431
Lognormal	μ	-0.117588	-0.370807	-0.527378
	σ	0.0313482	0.0569844	0.0916859
Nakagami	μ	258.046	78.2422	29.7141
	ω	0.791966	0.479405	0.354221
Normal	μ	0.889494	0.691284	0.59263
	σ	0.0278658	0.0393723	0.0552151
Rayleigh	b	0.629272	0.489594	0.420845
Rician	s	0.889062	0.690172	0.590061
	σ	0.0277	0.0391602	0.0549937
Weibull	a	0.902937	0.709917	0.618425
	b	33.8594	19.0386	10.5771

Table 8. Results of the Kolmogorov-Smirnov goodness-of-fit test for DoB sample 1 (Crown position−1st IPB loading).

Fitted distribution	Test statistic (d_n)	Critical value ($D_{n,\xi}$)		Test result	
		ξ = 0.05	ξ = 0.01	ξ = 0.05	ξ = 0.01
Beta	0.046707	0.1509	0.180844444	Accept	Accept
Birnbaum-Saunders	0.054485			Accept	Accept
Extreme Value	0.073507			Accept	Accept
Gamma	0.054384			Accept	Accept
Generalized Extreme Value	0.050741			Accept	Accept
Inverse Gaussian	NaN			-	-
Log-logistic	0.060637			Accept	Accept
Lognormal	0.053002			Accept	Accept
Nakagami	0.054241			Accept	Accept
Normal	0.0526			Accept	Accept
Rayleigh	0.575706			Reject	Reject
Rician	0.054097			Accept	Accept
Weibull	0.067876			Accept	Accept

Table 9. Best-fitted distributions for the DoB samples at the crown position of the central brace based on the results of the Kolmogorov-Smirnov test.

Best-fitted distributions	DoB samples		
	Sample 1 (1st IPB load case)	Sample 2 (2nd IPB load case)	Sample 3 (3rd IPB load case)
#1	Beta	Lognormal	Log-logistic
#2	Generalized Extreme Value	Inverse Gaussian	Generalized Extreme Value
#3	Normal	Birnbaum-Saunders	Lognormal

Table 10. Comparison of the test statistics for the proposed and the best-fitted distributions based on the results of the Kolmogorov-Smirnov test (Crown position of the central brace DoB samples).

	Test statistic		
	Sample 1 (1st IPB load case)	Sample 2 (2nd IPB load case)	Sample 3 (3rd IPB load case)
Best-fitted distribution	0.046707 (Beta)	0.069696 (Lognormal)	0.065531 (Log-logistic)
Proposed distribution	0.050741 (Generalized Extreme Value)	0.080025 (Generalized Extreme Value)	0.068212 (Generalized Extreme Value)
Difference	8.64%	14.82%	4.09%

Table 11. Comparison of the test statistics for the proposed and the best-fitted distributions based on the results of the Kolmogorov-Smirnov test (Toe position of the outer brace DoB samples).

	Test statistic		
	Sample 4 (1st IPB load case)	Sample 5 (2nd IPB load case)	Sample 6 (3rd IPB load case)
Best-fitted distribution	0.106385 (Extreme Value)	0.08399 (Generalized Extreme Value)	0.116099 (Extreme Value)
Proposed distribution	0.110175 (Generalized Extreme Value)	0.08399 (Generalized Extreme Value)	0.116984 (Generalized Extreme Value)
Difference	3.56%	0%	0.76%

Table 12. Comparison of the test statistics for the proposed and the best-fitted distributions based on the results of the Kolmogorov-Smirnov test (Heel position of the outer brace DoB samples).

	Test statistic		
	Sample 7 (1st IPB load case)	Sample 8 (2nd IPB load case)	Sample 9 (3rd IPB load case)
Best-fitted distribution	0.046671 (Generalized Extreme Value)	0.046882 (Generalized Extreme Value)	0.049635 (Generalized Extreme Value)
Proposed distribution	0.046671 (Generalized Extreme Value)	0.046882 (Generalized Extreme Value)	0.049635 (Generalized Extreme Value)
Difference	0%	0%	0%